scientific reports

Check for updates

OPEN

Modeling of three dimensional Prandtl hybrid nano-material over a heated rotating cone involving hall and ion slip currents via finite element procedure

Muhammad Sohail[1], Umar Nazir[2], Essam R. El-Zahar[3,4], Choonkil Park[5], Kanit Mukdasai[6]✉ & Amjad Iqbal[7]

Flow in a rotating cone for magnetized Prandtl fluid model is inspected in this investigation. The momentum equation of Prandtl model is derived under the consideration of Hall and ion slip effects and heat transport phenomenon is considered with Joule heating and viscous dissipation effects. The model of Hamilton Crosser and Yamada Ota are considered for the empirical relations of nanofluid mixture. The flow presenting expression of Prandtl fluid model with thermal transport is modeled under boundary layer approximation in the form of partial differential equations (PDEs). The derived PDEs have been converted into set of coupled nonlinear ordinary differential equations (ODEs) by engaging an appropriate scaling group transformation and these converted nonlinear set of ODEs have been tackled numerically via finite element scheme (FES). Impact of different emerging parameters has been displayed graphically and the physics behind the observed phenomena is explained in detail. The convergence of FES is established by carrying the grid independent survey. From the performed investigation, it is recorded that the parameters appear due to Hall and Ion slip currents enhance the fluid velocity but the inverse behavior is recorded for temperature profile.

List of symbols

τ^*	Stress tensor (N m^{-2})
$\widetilde{u}$, $\widetilde{w}$, $\widetilde{v}$	Velocity components (m s^{-1})
Ω	Rotating velocity (m s^{-1})
β	Thermal expansion coefficient (K^{-1})
T_∞	Ambient temperature (K)
σ	Electrical conductivity (S m^{-1})
β_i	Ion slip number (–)
ρ	Fluid density (kg m^{-3})
k	Thermal conductivity (kg s^{-3} K^{-1} m)
ϕ_1, ϕ_2	Volume fractions for nanoparticles (–)
β, α	Fluid parameters (–)
M	Magnetic number (–)
H_s	Heat source number (–)
TiO_2	Titanium dioxide (–)
FEM	Finite element method (–)

[1]Department of Mathematics, Khwaja Fareed University of Engineering and Information Technology, Rahim Yar Khan 64200, Pakistan. [2]Department of Applied Mathematics and Statistics, Institute of Space Technology, P.O. Box 2750, Islamabad 44000, Pakistan. [3]Department of Mathematics, College of Science and Humanities in Al-Kharj, Prince Sattam Bin Abdulaziz University, P.O. Box 83, Al-Kharj 11942, Saudi Arabia. [4]Department of Basic Engineering Science, Faculty of Engineering, Menoufia University, Shebin El-Kom 32511, Egypt. [5]Research Institute for Natural Sciences, Hanyang University, Seoul 04763, Korea. [6]Department of Mathematics, Faculty of Science, Khon Kaen University, Khon Kaen 40002, Thailand. [7]Department of Materials Technologies, Faculty of Materials Engineering, Silesian University of Technology, 44-100 Gliwice, Poland. ✉email: kanit@kku.ac.th

Re	Reynolds number (–)
C_f	Skin friction coefficient
PDEs	Partial differential equations
a^*, c^*	Material constants (–)
x, z	Space coordinates (m)
g	Gravitational acceleration (ms^{-2})
T	Fluid temperature (K)
β_0	Magnitude of magnetic field (Am^{-1})
β_e	Hall parameter (–)
ν	Kinematic viscosity ($m^2\ s^{-1}$)
C_p	Specific heat capacity ($J\ kg^{-1}\ K$)
Q	Heat source (J)
λ	Mixed convection number (–)
Pr	Prandtl number (–)
Ec	Eckert number (–)
$C_2H_6O_2$	Ethylene glycol (–)
SiO_2	Silicon dioxide (–)
θ, f, g	Dimensionless temperature and velocities (–)
NU	Nusselt number (–)
η	Independent variable
ODEs	Ordinary differential equations

The study of non-Newtonian fluids got much attention due to their applications in numerous field of applied sciences and engineering. An important non-Newtonian model is Prandtl fluid. Due to application in different mechanisms several researchers have worked on it. The constitutive relation for Prandtl model is

$$\tau^* = a^*\left[\left(\frac{\partial u}{\partial z}\right)^2 + \left(\frac{\partial v}{\partial z}\right)^2\right]^{-\frac{1}{2}} \sin^{-1}\left[c^*\left(\left(\frac{\partial u}{\partial z}\right)^2 + \left(\frac{\partial v}{\partial z}\right)^2\right)^{\frac{1}{2}}\right] \tag{1}$$

where "τ^*" denotes the stress tensor for Prandtl model and "a^*, c^*" are material constants. Several researchers have worked on Prandtl model with different effects. For instance, Hamid et al.[1] studied numerically the time dependent radiated Prandtl model with thermal and solutal transportation obeying slip mechanism. They used finite difference procedure to solve the modeled equations numerically in MAPLE package. They monitored the escalation in fluid velocity, concentration, and temperature fields respectively against unsteadiness parameter. Akbar et al.[2] worked on peristaltic transport phenomenon in Prandtl model in an asymmetric channel and handled the arising modeled equations via perturbation scheme. They used a numerical procedure as well for the comparison purpose and presented the tabulated study for the authenticity of obtained solution. They reported the excellent agreement in perturbation solution and numerical solution. They found the decrease in pressure rise against fluid parameter and phase difference. Muser[3] presented the rheology of Prandtl model in different physical effects under different conditions and recorded the nature of Prandtl model in various situations. Garaud[4] presented an experimental investigation for double diffusion phenomenon under low Prandtl number assumption. Nadeem et al.[5] analyzed endoscope while studying peristaltic transport in Prandtl model and monitored the numerous patterns of waves. They computed the solution of modeled equations analytically via perturbation tool. Perturbation solution is computed by Munawar[6] and analyzed the phenomenon of peristaltic transport in a channel. They noticed the decrease in fluid velocity against magnetic parameter.

The transport phenomenon can be enhanced by mixing the nanoparticles in base fluid. The study of nanofluids is important due to their significant applications in different processes. The study of nanofluids is a charming field of research due to huge applications in different industrial processes. Several researchers have considered nanofluids in their research due to their practical applications and usage. For instance, Das et al.[7] presented a review of nanofluids with their applications focusing on thermal transport. Godson et al.[8] presented a survey on escalation in heat transfer using nanofluids in different processes. Daungthongsuk and Wongwises[9] presented experimental and theoretical survey on convection and enhancement in thermal transport utilizing nanofluids mixture. Vanaki et al.[10] presented a numerical investigation on heat transport in nanofluids with numerous introduced models and discuss about the thermo-physical features. In another exploration, Solangi et al.[11] worked on a comprehensive review of nanofluid and explored their properties and preparation mechanism. Also, they highlighted the importance and utilization of nanofluids. Mansour et al.[12] worked on forced convective thermal transportation in nanofluids. Lomascolo et al.[13] presented an experimental investigation on thermal transportation in nanofluids and presented the different heat transport modes and expressed their significance. Kim et al.[14] studied the utilization of nanoparticles in different systems and monitored the boiling effect. Fard et al.[15] presented the CFD analysis for single phase and two phase nanofluid model in a tube and monitored the comparative heating efficiency. The phenomenon of heating is improved by including the carbon nanotubes in nanofluid modelling was reported by Marquis and Chibante[16]. Several important contributions on nanofluid are covered in[17–20]. Ayub et al.[21] studied cross nanomaterial in the presence of stagnation point flow inserted magnetic field using velocity slip phenomena. Shah et al.[22] investigated several features regarding Carreau liquid using approach of nanoparticles under influence of magnetic parameter over wedge. Ayub et al.[23] discussed several thermal aspects of Carreau liquid involving influence of magnetic field. Shah et al.[24] captured chemical species and heat energy characteristics in Cross nanofluid inserting an impact of magnetic dipole in cylindrical

panels. Ayub et al.[25] discussed thermal features of Cross fluid considering effects of thermal radiation and Lorentz force using 3D rotating disks. Ayub et al.[26] studied impacts of hybrid nanomaterial using nanoscale energy phenomena in the presence of magnetic field via Lobatto IIIA approach. Shah et al.[27] estimated heat energy features of cross fluid inserted approach of nanoparticles on heated surface using cubic autocatalysis. Chamkha and Al-Mudhaf[28] estimated influences of Lorentz force in mass diffusion and thermal energy in the presence of heat source in rotating cone. Takhar et al.[29] discussed characterizations of time dependent flow using Lorentz force in energy transfer in heating cone. Reddy et al.[30] captured features based on mass diffusion and thermal energy in the presence of chemical reaction involving suspension of nanoparticles in base fluid past a porous cone. Chamkha[31] studied influences of Lorentz force using concept of Hall force in energy transfer phenomena over porous plate. Takhar et al.[32] captured role of mass diffusion and heat energy in moving cylinder considering bouncy force. Relevant studies are mentioned in[33–42]. Parveen et al.[43] studied an inclination in energy transfer using thermal radiation and Lorentz force occurring hybrid nanomaterial via entropy generation. Shoaib et al.[44] studied numerical impacts of Lorentz force in 3D flow in the presence of viscous dissipation and hybrid nanomaterial in rotational disk via used Lobatto IIIA approach. Parveen et al.[45] studied properties of microorganisms in rheology of peristaltic liquid in the occurrence of Joule heating using nanoparticles. Awais et al.[46] estimated immersion of nanoparticles in bio-convective flow using concept of viscous dissipations and heat immersion. Khan et al.[47] observed thermal features of second law analysis occurring viscous dissipation and mixed convection flow. Relevant studies are mentioned in[48–54].

Available literature shows that no study is performed on three dimensional Prandtl model covering Hall effect with Hamilton Crosser and Yamada Ota model by finite element scheme. This attempt fills this gap. This paper is organized in five sections. A comprehensive review of literature is included in "Introduction", modeling of Prandtl model in rotating frame under numerous important physical effects is covered in section "Development regarding flow analysis" with dimensionless procedure arising nonlinear boundary value problem is tackled in section "Numerical technique", and the scheme is implemented and explained in detail; obtained graphical and tabular results are analyzed and explained in section "Outcomes and discussion" and important findings are covered in section "Prime consequences".

Development regarding flow analysis

Consider the thermal performance of ethylene glycol of 3D Prandtl fluid of nanoparticles and hybrid nanoparticles over a cone rotating with angular velocity. Models regarding Hamilton crosser and Yamada Ota are inserted. The wall temperature is considered to be non-uniform. Further, the effects of Hall, heat source and ion forces are taken to be significant and the concept of buoyancy forces is generated due to force of gravity. The flow of viscous fluid is induced due to rotating of heated cone. MoS_2–SiO_2-ethylene glycol is considered as plasma and shear thinning. The set of PDEs are obtained using basic laws under boundary layer approximations. The following effects have been considered in PDEs while modeling the flow over a rotating cone.

- Stress tensor of Prandtl fluid is used in desired PDEs;
- The concept of Hall and ion slip forces are considered;
- 3D rotating flow in heated cone is visualized;
- Bouncy force and Lorentz force are addressed;
- Joule heating and heat source are implemented;
- Hamilton Crosser and Yamada Ota models for hybrid nanofluid are considered;
- Thermal properties of ethylene glycol, titanium dioxide and silicone dioxide are assumed.

The direction of gravitational acceleration is considered downward in direction of axis via cone. Z-axis is normal component of cone and motion of particles is rotated with angular velocity Ω. Temperature at away of wall and for a way of wall is considered as T_w and T_∞. The velocity components $\widetilde{w}$, $\widetilde{u}$ and $\widetilde{v}$ along z, x and $y-$ directions. The physical flow model is captured by Fig. 1.

$$\frac{\partial(x\widetilde{u})}{\partial x}+\frac{\partial(x\widetilde{v})}{\partial z}=0, \tag{2}$$

$$\begin{aligned}\widetilde{u}\frac{\partial\widetilde{u}}{\partial x}+\widetilde{w}\frac{\partial\widetilde{u}}{\partial z}=\frac{(\widetilde{v})^2}{x}+\nu_{hnf}\left(\frac{A}{C}\frac{\partial^2\widetilde{u}}{\partial z^2}+\frac{A}{2C^3}\left(\frac{\partial\widetilde{u}}{\partial z}\right)^2\frac{\partial^2\widetilde{u}}{\partial z^2}\right)+g\beta(T-T_\infty)\cos\alpha\\+\frac{(B_0)^2\sigma_{hnf}}{\rho_{hnf}\left[(1+\beta_i\beta_e)^2+(\beta_e)^2\right]}\left[\widetilde{v}\beta_e-(1+\beta_e\beta_i)\widetilde{u}\right],\end{aligned} \tag{3}$$

$$\begin{aligned}\widetilde{u}\frac{\partial\widetilde{v}}{\partial x}+\widetilde{w}\frac{\partial\widetilde{v}}{\partial z}=-\frac{\widetilde{v}\widetilde{u}}{x}+\nu_{hnf}\left(\frac{A}{C}\frac{\partial^2\widetilde{v}}{\partial z^2}+\frac{A}{2C^3}\left(\frac{\partial\widetilde{v}}{\partial z}\right)^2\frac{\partial^2\widetilde{v}}{\partial z^2}\right)\\-\frac{(B_0)^2\sigma_{hnf}}{\rho_{hnf}\left[(1+\beta_i\beta_e)^2+(\beta_e)^2\right]}\left[\widetilde{u}\beta_e+(1+\beta_e\beta_i)\widetilde{v}\right],\end{aligned} \tag{4}$$

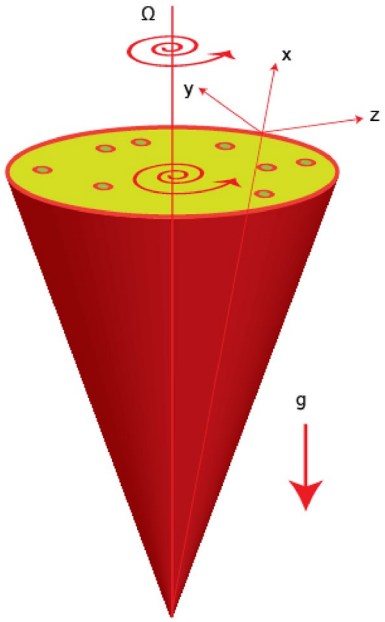

Figure 1. Rotating cone for developed problem.

	k (thermal conductivity)	C_p (heat capacity)	ρ (density)
$C_2H_6O_2$	0.253	2430	1113.5
TiO_2	8.4	692	4230
SiO_2	1.4013	3.5×10^6	2270

Table 1. Thermal properties for density (ρ), heat capacity (C_p) and thermal conductivity (k)[12].

$$\widetilde{u}\frac{\partial T}{\partial x}+\widetilde{w}\frac{\partial T}{\partial z}=\frac{k_{hnf}}{(\rho C_p)_{hnf}}\frac{\partial^2 T}{\partial z^2}+\frac{(\beta_0)^2\sigma_{hnf}}{(\rho C_p)_{hnf}\left[(1+\beta_i\beta_e)^2+(\beta_e)^2\right]}\left[(\widetilde{u})^2+(\widetilde{v})^2\right]+\frac{Q}{(\rho C_p)_{hnf}}(T-T_\infty). \tag{5}$$

The boundary conditions at wall and away from of wall are generated due to no-slip theory

$$\widetilde{u}=0,\ T=T_w,\ \widetilde{v}=\Omega x\sin\alpha,\ \widetilde{u}\to 0,\ \widetilde{v}\to 0,\ T\to T_\infty. \tag{6}$$

Transformations are defined as

$$\widetilde{u}=-\frac{\Omega x\sin\alpha f'}{2},\ \widetilde{v}=\Omega x\sin\alpha g,\ \widetilde{w}=\left(\nu_f\Omega\sin\alpha\right)^{\frac{1}{2}}f,\ T=T_\infty+(T_w-T_\infty)\theta,\ \eta=z\left(\frac{\Omega\sin\alpha}{\nu_f}\right)^{\frac{1}{2}}. \tag{7}$$

Correlations insight into nanoparticles and hybrid nanoparticles are mentioned below and physical properties are listed in Table 1.

$$\left.\begin{aligned}&\rho_{hnf}=\left[(1-\varnothing_2)\left\{(1-\varnothing_1)\rho_f+\varnothing_1\rho_{s1}\right\}\right]+\varnothing_2\rho_{s2}\\&(\rho C_p)_{hnf}=\left[(1-\varnothing_2)\left\{\begin{array}{c}(1-\varnothing_1)(\rho C_p)_f\\+\varnothing_1(\rho C_p)_{s1}\end{array}\right\}\right]+\varnothing_1(\rho C_p)_{s2}\\&\left\{\frac{k_{s1}+(n-1)k_f-(n-1)\varnothing_1(k_f-k_{s2})}{k_{s1}+(n-1)k_f-\varnothing_1(k_{s2}-k_f)}\right\}=\frac{k_{bf}}{k_f}\end{aligned}\right\}, \tag{8}$$

$$\left.\begin{aligned}
&\mu_{hnf} = \frac{(1-\varnothing_2)^{2.5}\mu_f}{(1-\varnothing_1)^{2.5}},\ \frac{k_{nf}}{k_f} = \left\{\frac{k_s+(n+1)k_f-(n-1)\varnothing\left(k_f-k_s\right)}{k_s+(n-1)k_f+\varnothing\left(k_f-k_s\right)}\right\}\\
&\frac{k_{hnf}}{k_{bf}} = \left\{\frac{k_{s2}+(n-1)k_{bf}-(1-n)\varnothing_2\left(k_{s2}-k_{bf}\right)}{k_{s2}+(n-1)k_{bf}-\varnothing_2\left(k_{bf}-k_{s2}\right)}\right\}\\
&\left\{\frac{k_{s2}+(n-1)k_{bf}-(1-n)\phi_2\left(k_{s2}-k_{bf}\right)}{k_{s2}+(n-1)k_{bf}-\phi_2\left(k_{bf}-k_{s2}\right)}\right\} = \frac{k_{hnf}}{k_{bf}}
\end{aligned}\right\}, \tag{9}$$

$$\left.\begin{aligned}
&\frac{k_{hnf}}{k_{bf}} = \left\{\frac{\frac{k_{s2}}{k_{bf}}+\omega+\omega\emptyset_2\left(1-\frac{k_{s2}}{k_{bf}}\right)}{\frac{k_{s2}}{k_{bf}}+\omega+\emptyset_2\left(1-\frac{k_{s2}}{k_{bf}}\right)}\right\}\omega = 2\emptyset_2^{\frac{1}{5}}\frac{L}{D}\ \text{for cylindrical particle}\\
&\omega = 2\emptyset_2^{1/5}\text{for spherical particle}
\end{aligned}\right\}, \tag{10}$$

$$\left.\begin{aligned}
&\frac{k_{hnf}}{k_{bf}} = \left\{\frac{\frac{k_{s1}}{k_f}+\omega+\omega\emptyset_1\left(1-\frac{k_{s1}}{k_f}\right)}{\frac{k_{s1}}{k_f}+\omega+\emptyset_1\left(1-\frac{k_{s1}}{k_f}\right)}\right\}\omega = 2\emptyset_2^{\frac{1}{5}}\frac{L}{D}\ \text{for cylindrical particle}\\
&\omega = 2\emptyset_2^{1/5}\ \text{for spherical particles}
\end{aligned}\right\}. \tag{11}$$

Formulated ODEs are

$$\begin{aligned}
\frac{\nu_f}{\nu_{hnf}}\left(\frac{1}{2}\left(f'\right)^2 - ff'' - 2g^2 - 2\lambda\theta\right) - \frac{(1-\emptyset_1)^{2.5}M^2(1-\emptyset_2)^{2.5}}{\left[(1+\beta_i\beta_e)^2+(\beta_e)^2\right]}\left[2\beta_e g + (1+\beta_i\beta_e)f'\right]\\
+\alpha f''' + \beta\left(f''\right)^2 f''' = 0,
\end{aligned} \tag{12}$$

$$\begin{aligned}
\frac{\nu_f}{\nu_{hnf}}\left(gf' - f'g'\right) - \frac{(1-\emptyset_1)^{2.5}M^2(1-\emptyset_2)^{2.5}}{\left[(1+\beta_i\beta_e)^2+(\beta_e)^2\right]}\left[(1+\beta_i\beta_e)g - \frac{1}{2}\beta_e f'\right]\\
+\alpha g'' + \beta\left(g'\right)^2 g'' = 0,
\end{aligned} \tag{13}$$

$$\begin{aligned}
&\theta'' + \frac{k_f}{k_{hnf}}\frac{\left(\rho C_p\right)_{hnf}}{\left(\rho C_p\right)_f}Pr\left(\frac{1}{2}f'\theta - f\theta'\right) + \frac{k_f}{k_{hnf}}\frac{M^2 EcPr}{\left[(1+\beta_i\beta_e)^2+(\beta_e)^2\right]}\left(\frac{1}{4}f'^2 + g^2\right)\\
&+\frac{k_f}{k_{hnf}}H_s Pr\theta = 0.
\end{aligned} \tag{14}$$

Boundary conditions in term of dimensionless are

$$f'(0) = 0,\ f'(\infty) = 0,\ g(0) = 1,\ g(\infty) = 0,\ \theta(\infty) = 0,\ f(0) = 0,\ \theta(0) = 1. \tag{15}$$

Dimensionless parameters utilized in Eqs. (12) and (14) are defined as

$$\begin{aligned}
&Pr = \frac{\left(C_p\right)_f\mu_f}{k_f}, M^2 = \frac{(\beta_0)^2\sigma_{nf}}{\rho_f\Omega\sin\alpha_1}, Ec = \frac{(U_w)^2}{(T_w-T_\infty)\left(C_p\right)_f}, \lambda = \frac{gL\beta\cos\alpha_1}{\left(\nu_f\right)^2\Omega\sin\alpha_1},\\
&H_s = \frac{Q}{\Omega sin\alpha_1\left(\rho C_p\right)_f}, \alpha = \frac{1}{A\mu_f C}, \beta = \frac{\Omega(U_w)^2}{2\nu_f C^2}.
\end{aligned}$$

Divergence of velocity along horizontal and vertical direction is

$$(Re)^{\frac{1}{2}}C_f = \frac{-\left[\alpha f''(0) + \beta\left(f'''(0)\right)^3\right]}{(1-\emptyset_1)^{2.5}(1-\emptyset_2)^{2.5}},\quad (Re)^{\frac{1}{2}}C_g = \frac{-\left[\alpha g'(0) + \beta\left(g''(0)\right)^3\right]}{(1-\emptyset_1)^{2.5}(1-\emptyset_2)^{2.5}}. \tag{16}$$

The mathematical relation for temperature gradient (Nusselt number) is

$$(Re)^{\frac{-1}{2}}NU = \frac{-k_{hnf}}{k_f}\theta'(0). \tag{17}$$

Numerical technique

The numerical approach is adopted as a finite element scheme[52] (FEM)[17,18] to compute the solution of highly ODEs (non-linear). The domain of current model is broken into small segments called finite element scheme. The applications of FEM are used in electrical systems, solid mechanics, chemical processing and fluid related problems etc. The solution related steps of FEM is listed below.

Number of elements	$f'\left(\frac{\eta_{max}}{2}\right)$	$g\left(\frac{\eta_{max}}{2}\right)$	$\theta\left(\frac{\eta_{max}}{2}\right)$
30	0.6586386817	0.0001721355025	0.6605821625
60	0.6233792179	0.6437292447	0.0002229082388
90	0.6116725178	0.6380761926	0.0002319259575
120	0.6058311283	0.6352430888	0.0002348216628
150	0.6023296966	0.6335412345	0.0002360353595
180	0.5999974251	0.6324058465	0.0002366270036
210	0.5983324921	0.6315945612	0.0002369433746
240	0.5970846646	0.6309857193	0.0002371243282
270	0.5961135026	0.6305118421	0.0002372274024
300	0.5953371601	0.6301329244	0.0002372898241

Table 2. Simulations of mesh free analysis for velocities and temperature when $\emptyset_1 = 0.002, \emptyset_2 = 0.0075$, $\lambda = 0.3, \beta_e = 0.3, \alpha = 2.0, \beta_i = 0.002, \beta = 0.2, Pr = 206, Ec = 3.2, H_s = 0.2, M = 0.01$.

	Present work			Malik et al.[54]		
λ	$-(Re)^{\frac{1}{2}} C_f$	$-(Re)^{\frac{1}{2}} C_g$	$-(Re)^{\frac{-1}{2}} NU$	$-(Re)^{\frac{1}{2}} C_f$	$-(Re)^{\frac{1}{2}} C_g$	$-(Re)^{\frac{-1}{2}} NU$
0.0	0.6330341643	0.6153201962	0.4295412140	1.0253	0.6153	0.4295
1.0	2.2006812241	0.8492300251	0.6128301282	2.2007	0.8492	0.6121
10	8.5982303219	1.3993024924	1.009332492	8.5041	1.3990	1.0097

Table 3. Validation in view of numerical behavior for flow rates and temperature gradient when $\emptyset_1 = \emptyset_2 = 0.0, \beta_e = 0.0, \alpha = 2.0, \beta_i = 0.0, \beta = 0.2, Pr = 0.7, Ec = 0.0, H_s = 0.0$.

Step-I: Weak form is made from strong form (said ODEs) and residuals are formulated;
Step-II: Shape functions are taken as linearly and Galerkin finite element scheme is utilized to obtain weak form;
Step-III: Assembly process is utilized to construct stiffness elements and global stiffness matrix is formulated;
Step-IV: Algebraic system (nonlinear equations) is obtained with help of Picard linearization approach;
Step-V: Algebraic equations are simulated via 10^{-5} (computational tolerance) using following stopping criteria;

$$\left|\frac{X_{i+1} - X_i}{X^i}\right| < 10^{-5}. \tag{18}$$

Step-VI: Table 2 reveals investigation of mesh-free;
Step-VII: Convergence analysis is confirmed via 300 elements.

Validation of problem. Code and problem are validated in case of Nusselt number and flow rates with published work. It can be estimated that good agreements are simulated between published work and present problem by disappearing impacts of ion slip, Hall current, heat sink and viscous dissipation in current problem. This validation is recorded in Table 3.

Outcomes and discussion

Modeled equations are solved via FEM and parametric analysis is carried out in order to examine transport of momentum and heat.

Outcomes of velocity fields. The solid curves are for velocity components of Yamada Ota model whereas dot curves are for velocity components of Hamilton Crosser hybrid nanomaterial model. An influence of α on flow distribution in both components is carried out by Fig. 2a,b. It is noticed that parameter related to α is formulated due to appearance of Prandtl rheology in momentum equations. Mathematically, directly proportional relation is investigated between velocity curves and fluid number. Therefore, flow is produced slowly down versus implication of α. Hence, viscosity of fluid is increased when fluid number is increased. Thickness for momentum layers is also declined against change in α. Flow produced by Yamada Ota model is higher than flow produced by Hamilton Crosser hybrid nanomaterial model. Figures 3a,b, 4a,b reveal influences of ion slip number (β_i) and Hall number (β_e) on flow components in y- and x-directions. It is observed that ion slip and Hall currents are produced using concept of generalized Ohm's law in current problem. In mathematically, flow distributions have direct proportional relation against β_e and β_i. Therefore, argumentation insight into fluidic particles is predicted against implication of β_e and β_i. Physically, (β_i) ion slip number is produced by product among ion cyclotron frequency and ion collision time. An increment into ion slip number produces an inclination into ion cyclotron frequency and ion collision time. This physical reason is produced an enhancement into

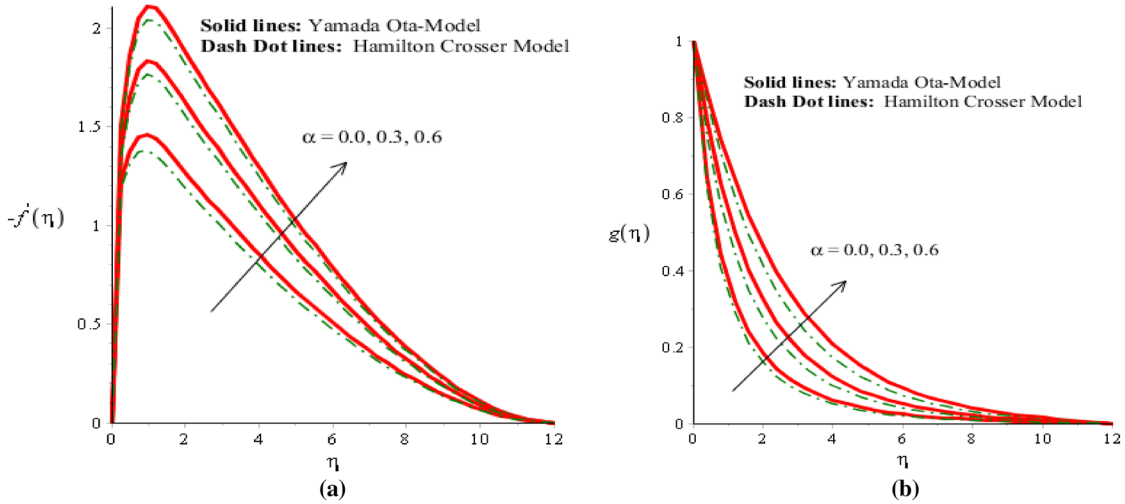

Figure 2. (**a**,**b**) Velocity field in y-direction and x-direction against α when $\emptyset_1 = 0.002, \emptyset_2 = 0.0075$, $\lambda = 2.0, \beta_e = 0.2, \beta_i = 0.01, \beta = 0.3, Pr = 206, Ec = 2.2, H_s = -0.2, M = 0.03$.

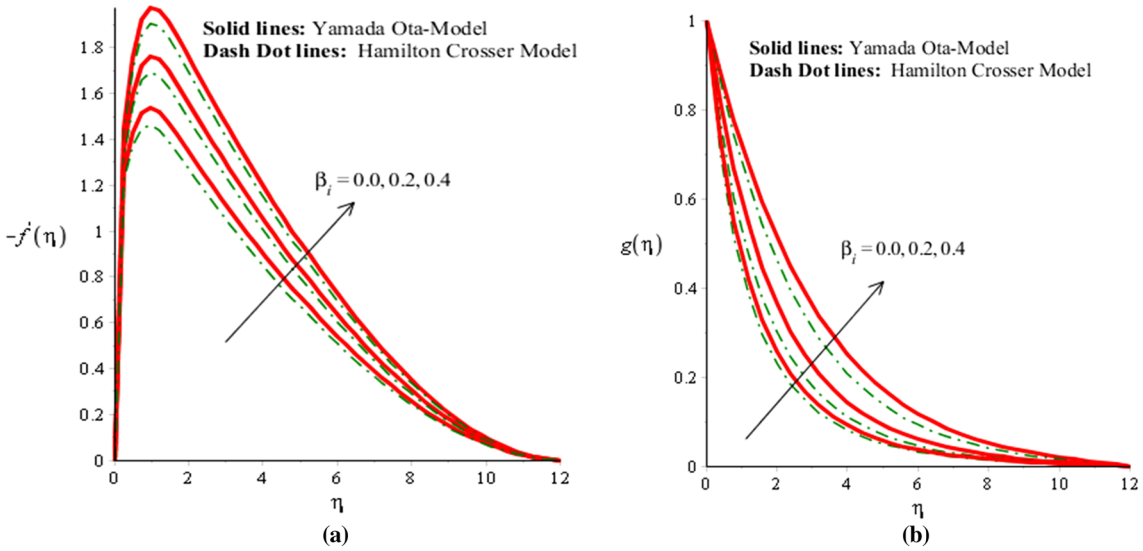

Figure 3. (**a**,**b**) Velocity field in y-direction and x-direction against β_i when $\emptyset_1 = 0.002, \emptyset_2 = 0.0075$, $\lambda = 0.3, \beta_e = 2.0, \alpha = 2.0, \beta = 00.2, Pr = 206, Ec = 3.0, H_s = 2.0, M = 0.3$.

motion regarding both directions. Velocity curves are significantly increased for Yamada Ota model rather than Hamilton Crosser hybrid nanomaterial model. It is noted through the impact of Hall and ion slip currents on velocity in case of ethylene glycol are displayed. The flow of ethylene glycol is funded to be plasma and exposed to be applied magnetic field. Hall and ion forces are generated due to the interaction of plasma and applied magnetic field. The Lorentz force is reduced due to an increase in Hall and ion slip parameters. This fact is because of Hall, ion forces and magnetic field are opposite which are responsible reduction in Lorentz force. The flow is accelerated because of Hall and ion forces for both cases of nanofluids and hybrid nanofluids. Due to opposite behavior among Lorentz force and ion slip and Hall forces, flow was enhanced and momentum thickness was also enhanced when Lorentz force was declined. This impact of Hall and ion slip currents on the flow is observed. Hence, Yamada Ota hybrid nano-metallic particles should be dispersed in pure fluid is recommended for its better thermal performance rather than Hamilton Crosser hybrid model.

Outcomes of temperature field. The solid curves are for velocity components of Yamada Ota model whereas dot curves are for velocity components of Hamilton Crosser hybrid nanomaterial model. It is included that an efficiency of Yamada Ota model increases rather than the ethylene glycol regarding Hamilton Crosser hybrid nanomaterial model. Figure 5 demonstrates impact of Eckert number on thermal distribution. It is

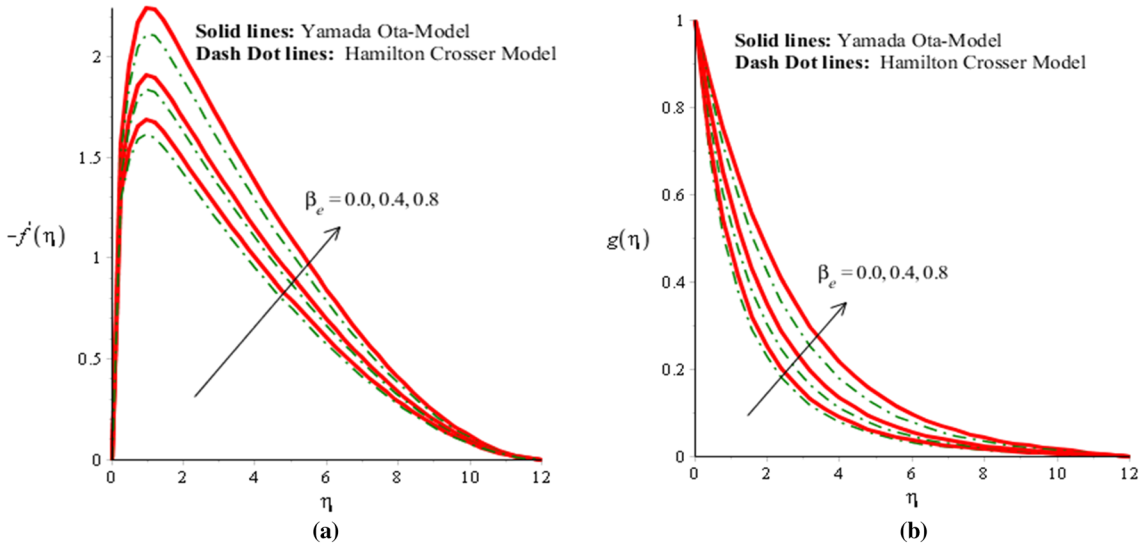

Figure 4. (**a**,**b**) Velocity field in y-direction and x-direction against β_i when $\emptyset_1 = 0.002, \emptyset_2 = 0.0075$, $\lambda = 2.3, \alpha = 2.0, \beta_i = 0.02, \beta = 2, Pr = 206, Ec = 0.1, H_s = 0.4, M = 0.3$.

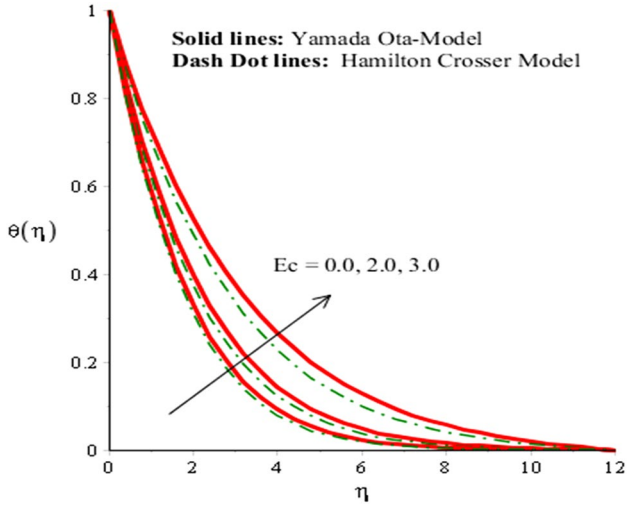

Figure 5. Analysis of heat energy field in against Ec when $\emptyset_1 = 0.002, \emptyset_2 = 0.0075, \lambda = 0.3, \beta_e = 0.4$, $\alpha = 3.0, \beta_i = 2.0, \beta = 0.2, Pr = 206, H_s = -3.0, M = 0.03$.

noticed that Ec is produced using concept of viscous dissipation into energy equation. It is coefficient of joule heat and viscous dissipation. An inclination in Ec results heat energy is significantly dissipated because of friction force and Joule heating. Heat energy adds into fluid particles because of frictional force. Hence, temperature is increased. Furthermore, thermal layers thickness for case of Yamada Ota hybrid nanomaterial model is higher than for case of Hamilton Crosser hybrid nanomaterial model. Figure 6 represents role of H_s (heat source number) on thermal profile. Two type's influences were conducted into fluidic particles which are based on heat absorption and heat generation. External thermal source was placed at wall. So, thermal energy can be managed using variation of H_s. Hence, Yamada Ota hybrid nanomaterial model in ethylene glycol is recommended for its better thermal performance rather than Hamilton Crosser hybrid nanomaterial model. Additionally, heat is generated due to enhancement in Eckert number. This fact is due to Ec acts as coefficient of viscous dissipation term. Therefore, more heat is produced due friction between the fluid particles. The role of Hall and ion-slip numbers on the temperature for both cases of two hybrid models in Figs. 7 and 8. However, temperature decreases when ion slip and Hall parameters are increased via Hall and ion slip parameters because Hall and ion slip currents play a key role in a controlling the dissipation of heat energy. Physically, collision into electron and ions are called ion slip and Hall forces. The direction among magnetic field and applied Lorentz force is opposite. Therefore, Lorentz force decreases when β_i and β_e are increased. Hence, TBLT (thermal boundary layer thickness) can be shortened via external magnetic field and use fluid in plasma state.

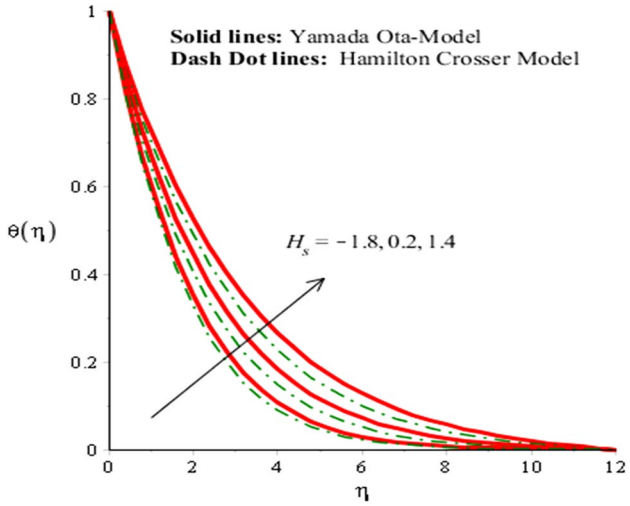

Figure 6. Analysis of heat energy field in against H_s when $\emptyset_1 = 0.002, \emptyset_2 = 0.0075, \lambda = 0.3, \beta_e = 0.3, \alpha = 2.0, \beta_i = 0.2, \beta = 0.9, Pr = 206, Ec = 3, M = 0.01$.

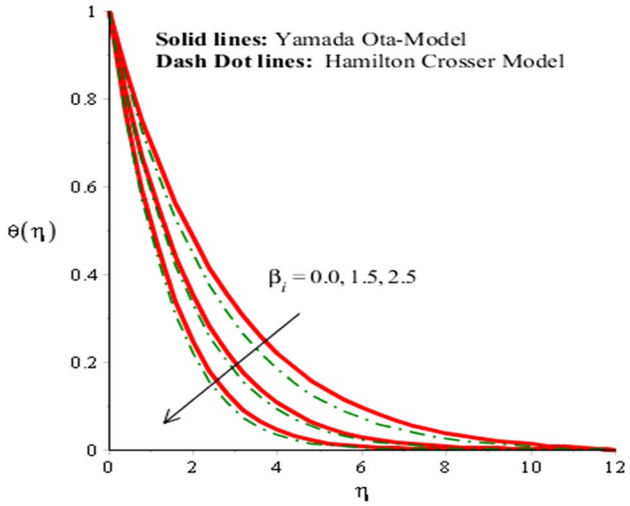

Figure 7. Analysis of heat energy field in against β_i when $\emptyset_1 = 0.002, \emptyset_2 = 0.0075, \lambda = 4.0, \beta_e = 0.3, \alpha = 2.0, \beta = 0.2, Pr = 206, Ec = 4.0, H_s = 0.2, M = 2.0$.

Investigation regarding skin friction and Nusselt number. The impacts of M, β_e, β_i and H_s on the behavior skin friction coefficients and heat energy rate is observed and noted numerical values are displayed in Table 4. Magnetic field parameter has shown an increasing impact on wall shear stresses. But heat energy rate was decreased when Lorentz force is significantly enhanced. It is noted through shear stresses increase when β_e is increased whereas β_e is responsible for significant decrease in shear stress but more heat generates due to β_e into particles. Heat flux of mono-nanofluid and hybrid nanofluid decreases when heat source number is enhanced. However, the impact of shear stresses is decreased due to an increase in H_s.

Prime consequences

The ethylene glycol containing hybrid nano-structures subjected to magnetic field helps to use magneto-hydrodynamic equations to model the transportation of momentum and heat. Heat source is accumulated in the presence of Hamilton crosser and Yamada Ota models. Numerical solutions are computed via FEM and key outcomes are recorded which are listed here.

- Hall and ion slip currents help to accelerated flow in both x and y directions. However, temperature decreases when Hall and ion currents are increased because of Hall and ion slip currents play a key role in a controlling

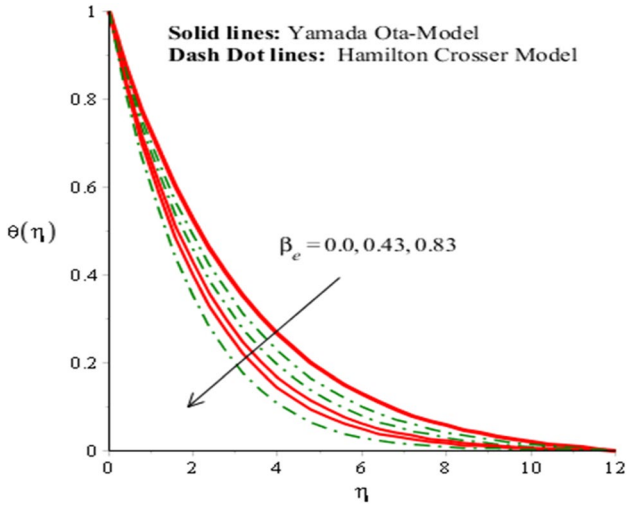

Figure 8. Analysis of heat energy field in against β_e when $\emptyset_1 = 0.002, \emptyset_2 = 0.0075, \lambda = 0.3, \alpha = 2.0$, $\beta_i = 0.002, \beta = 0.8, Pr = 206, Ec = 3.2, H_s = 0.2, M = 0.01$.

Change in parameters		$(Re)^{\frac{1}{2}} C_f$	$(Re)^{\frac{1}{2}} C_g$	$(Re)^{\frac{1}{2}} NU$
M	0.0	0.5553481694	1.748625433	0.7829754254
	0.3	0.6552943007	1.754302238	0.7237240327
	0.6	0.7551674911	1.783088915	0.7161334864
β_e	0.0	0.5553328293	1.748062602	0.7831495083
	0.4	0.4553404122	1.648160325	0.8830709949
	0.8	0.3553430627	1.628288537	0.9830395354
H_s	-1.8	0.5160815058	1.659381887	0.794817722
	0.4	0.4011296359	1.518494450	0.674217273
	0.8	0.3943834879	1.509256446	0.410370366
β_i	0.0	0.5555095192	1.746942157	0.7606163594
	0.5	0.4555101361	1.647591937	0.8606106152
	1.7	0.3555110713	1.617968095	0.9605989369

Table 4. Numerical impacts of skin friction coefficients and heat transfer rate versus β_e, β_i, H_s and M when $\emptyset_1 = 0.002, \emptyset_2 = 0.0075, \lambda = 2.0, \beta_i = 0.01, \beta = 0.3, Pr = 206, Ec = 2.2$.

the dissipation of heat energy. Hence, the thermal boundary layer thickness can be controlled through the external magnetic field used is in plasma state;

- Hybridity of nano-structures in plasma ethylene glycol exposed to magnetic field. It is noted through extensive numerical experiments that hybrid nano-structures increases the thermal performances of ethylene glycol relative to mono-nano-structures;
- Wall shear stress in x-direction in case of ethylene glycol mono-nanofluid is greater than the wall shear stress in x-direction for the case of hybrid nanofluid and vice versa for wall shear stress in y-direction.

Data availability

The datasets generated/produced during and/or analyzed during the current study/research are available from the corresponding author on reasonable request.

Received: 3 April 2022; Accepted: 12 July 2022
Published online: 16 July 2022

References

1. Hamid, M., Zubair, T., Usman, M., Khan, Z. H. & Wang, W. Natural convection effects on heat and mass transfer of slip flow of time-dependent Prandtl fluid. *J. Comput. Des. Eng.* **6**(4), 584–592 (2019).
2. Akbar, N. S., Nadeem, S. & Lee, C. Peristaltic flow of a Prandtl fluid model in an asymmetric channel. *Int. J. Phys. Sci.* **7**(5), 687–695 (2012).

3. Müser, M. H. Shear thinning in the Prandtl model and its relation to generalized Newtonian fluids. *Lubricants* **8**(4), 38 (2020).
4. Garaud, P. Double-diffusive convection at low Prandtl number. *Annu. Rev. Fluid Mech.* **50**, 275–298 (2018).
5. Nadeem, S., Sadaf, H. & Akbar, N. S. Analysis of peristaltic flow for a Prandtl fluid model in an endoscope. *J. Power Technol.* **94**(2), 1–11 (2014).
6. Munawar, S. Significance of slippage and electric field in mucociliary transport of biomagnetic fluid. *Lubricants* **9**(5), 48 (2021).
7. Das, S. K., Choi, S. U. & Patel, H. E. Heat transfer in nanofluids—A review. *Heat Transf. Eng.* **27**(10), 3–19 (2006).
8. Godson, L., Raja, B., Lal, D. M. & Wongwises, S. E. A. Enhancement of heat transfer using nanofluids—An overview. *Renew. Sustain. Energy Rev.* **14**(2), 629–641 (2010).
9. Daungthongsuk, W. & Wongwises, S. A critical review of convective heat transfer of nanofluids. *Renew. Sustain. Energy Rev.* **11**(5), 797–817 (2007).
10. Vanaki, S. M., Ganesan, P. & Mohammed, H. A. Numerical study of convective heat transfer of nanofluids: A review. *Renew. Sustain. Energy Rev.* **54**, 1212–1239 (2016).
11. Solangi, K. H. *et al.* A comprehensive review of thermo-physical properties and convective heat transfer to nanofluids. *Energy* **89**, 1065–1086 (2015).
12. Mansour, R. B., Galanis, N. & Nguyen, C. T. Effect of uncertainties in physical properties on forced convection heat transfer with nanofluids. *Appl. Therm. Eng.* **27**(1), 240–249 (2007).
13. Lomascolo, M., Colangelo, G., Milanese, M. & De Risi, A. Review of heat transfer in nanofluids: Conductive, convective and radiative experimental results. *Renew. Sustain. Energy Rev.* **43**, 1182–1198 (2015).
14. Kim, S. J., Bang, I. C., Buongiorno, J. & Hu, L. W. Effects of nanoparticle deposition on surface wettability influencing boiling heat transfer in nanofluids. *Appl. Phys. Lett.* **89**(15), 153107 (2006).
15. Fard, M. H., Esfahany, M. N. & Talaie, M. R. Numerical study of convective heat transfer of nanofluids in a circular tube two-phase model versus single-phase model. *Int. Commun. Heat Mass Transf.* **37**(1), 91–97 (2010).
16. Marquis, F. D. S. & Chibante, L. P. F. Improving the heat transfer of nanofluids and nanolubricants with carbon nanotubes. *Jom* **57**(12), 32–43 (2005).
17. Wang, F. *et al.* A Galerkin strategy for tri-hybridized mixture in ethylene glycol comprising variable diffusion and thermal conductivity using non-Fourier's theory. *Nanotechnol. Rev.* **11**(1), 834–845 (2022).
18. Algehyne, E. A. *et al.* Investigation of thermal performance of Maxwell hybrid nanofluid boundary value problem in vertical porous surface via finite element approach. *Sci. Rep.* **12**(1), 1–12 (2022).
19. Imran, N., Javed, M., Sohail, M., Thounthong, P. & Abdelmalek, Z. Theoretical exploration of thermal transportation with chemical reactions for Sutterby fluid model obeying peristaltic mechanism. *J. Mark. Res.* **9**(4), 7449–7459 (2020).
20. Sohail, M., Shah, Z., Tassaddiq, A., Kumam, P. & Roy, P. Entropy generation in MHD Casson fluid flow with variable heat conductance and thermal conductivity over non-linear bi-directional stretching surface. *Sci. Rep.* **10**(1), 1–16 (2020).
21. Ayub, A., Shah, S. Z. H., Sabir, Z., Rao, N. S., Sadat, R. & Ali, M. R. Spectral relaxation approach and velocity slip stagnation point flow of inclined magnetized cross-nanofluid with a quadratic multiple regression model. *Waves in Random and Complex Media*, 1–25 (2022).
22. Shah, S. Z. H. *et al.* Inclined magnetized and energy transportation aspect of infinite shear rate viscosity model of Carreau nanofluid with multiple features over wedge geometry. *Heat Transf.* **51**(2), 1622–1648 (2022).
23. Ayub, A. *et al.* Aspects of infinite shear rate viscosity and heat transport of magnetized Carreau nanofluid. *Eur. Phys. J. Plus* **137**(2), 1–17 (2022).
24. Shah, S. L., Ayub, A., Dehraj, S., Wahab, H. A., Sagayam, K. M., Ali, M. R., Sadat, R. & Sabir, Z. Magnetic dipole aspect of binary chemical reactive Cross nanofluid and heat transport over composite cylindrical panels. *Waves in Random and Complex Media*, 1–24 (2022).
25. Ayub, A. *et al.* Effects of homogeneous-heterogeneous and Lorentz forces on 3-D radiative magnetized cross nanofluid using two rotating disks. *Int. Commun. Heat Mass Transf.* **130**, 105778 (2022).
26. Ayub, A., Darvesh, A., Altamirano, G. C. & Sabir, Z. Nanoscale energy transport of inclined magnetized 3D hybrid nanofluid with Lobatto IIIA scheme. *Heat Transf.* **50**(7), 6465–6490 (2021).
27. Shah, S. Z. H. *et al.* Insight into the dynamics of time-dependent cross nanofluid on a melting surface subject to cubic autocatalysis. *Case Stud. Therm. Eng.* **27**, 101227 (2021).
28. Chamkha, A. J. & Al-Mudhaf, A. Unsteady heat and mass transfer from a rotating vertical cone with a magnetic field and heat generation or absorption effects. *Int. J. Therm. Sci.* **44**(3), 267–276 (2005).
29. Takhar, H. S., Chamkha, A. J. & Nath, G. Unsteady mixed convection flow from a rotating vertical cone with a magnetic field. *Heat Mass Transf.* **39**(4), 297–304 (2003).
30. Reddy, P. S., Sreedevi, P. & Chamkha, A. J. MHD boundary layer flow, heat and mass transfer analysis over a rotating disk through porous medium saturated by Cu-water and Ag-water nanofluid with chemical reaction. *Powder Technol.* **307**, 46–55 (2017).
31. Chamkha, A. J. MHD-free convection from a vertical plate embedded in a thermally stratified porous medium with Hall effects. *Appl. Math. Model.* **21**(10), 603–609 (1997).
32. Takhar, H. S., Chamkha, A. J. & Nath, G. Combined heat and mass transfer along a vertical moving cylinder with a free stream. *Heat Mass Transf.* **36**(3), 237–246 (2000).
33. Krishna, M. V., Ahamad, N. A. & Chamkha, A. J. Hall and ion slip effects on unsteady MHD free convective rotating flow through a saturated porous medium over an exponential accelerated plate. *Alex. Eng. J.* **59**(2), 565–577 (2020).
34. Krishna, M. V. & Chamkha, A. J. Hall and ion slip effects on MHD rotating flow of elastico-viscous fluid through porous medium. *Int. Commun. Heat Mass Transf.* **113**, 104494 (2020).
35. Krishna, M. V., Ahamad, N. A. & Chamkha, A. J. Hall and ion slip impacts on unsteady MHD convective rotating flow of heat generating/absorbing second grade fluid. *Alex. Eng. J.* **60**(1), 845–858 (2021).
36. Ramesh, G. K., Shehzad, S. A., Rauf, A. & Chamkha, A. J. Heat transport analysis of aluminum alloy and magnetite graphene oxide through permeable cylinder with heat source/sink. *Phys. Scr.* **95**(9), 095203 (2020).
37. Chamkha, A. J. Non-Darcy hydromagnetic free convection from a cone and a wedge in porous media. *Int. Commun. Heat Mass Transf.* **23**(6), 875–887 (1996).
38. Bhattacharyya, A., Seth, G. S., Kumar, R. & Chamkha, A. J. Simulation of Cattaneo–Christov heat flux on the flow of single and multi-walled carbon nanotubes between two stretchable coaxial rotating disks. *J. Therm. Anal. Calorim.* **139**(3), 1655–1670 (2020).
39. Chamkha, A. J., Dogonchi, A. S. & Ganji, D. D. Magneto-hydrodynamic flow and heat transfer of a hybrid nanofluid in a rotating system among two surfaces in the presence of thermal radiation and Joule heating. *AIP Adv.* **9**(2), 025103 (2019).
40. Ghalambaz, M., Behseresht, A., Behseresht, J. & Chamkha, A. Effects of nanoparticles diameter and concentration on natural convection of the Al_2O_3–water nanofluids considering variable thermal conductivity around a vertical cone in porous media. *Adv. Powder Technol.* **26**(1), 224–235 (2015).
41. Takhar, H. S., Chamkha, A. J. & Nath, G. MHD flow over a moving plate in a rotating fluid with magnetic field, Hall currents and free stream velocity. *Int. J. Eng. Sci.* **40**(13), 1511–1527 (2002).
42. Chamkha, A. J. & Rashad, A. M. Unsteady heat and mass transfer by MHD mixed convection flow from a rotating vertical cone with chemical reaction and Soret and Dufour effects. *Can. J. Chem. Eng.* **92**(4), 758–767 (2014).
43. Parveen, N. *et al.* Entropy generation analysis and radiated heat transfer in MHD (Al_2O_3-Cu/Water) hybrid nanofluid flow. *Micromachines* **12**(8), 887 (2021).

44. Shoaib, M. *et al.* Numerical analysis of 3-D MHD hybrid nanofluid over a rotational disk in presence of thermal radiation with Joule heating and viscous dissipation effects using Lobatto IIIA technique. *Alex. Eng. J.* **60**(4), 3605–3619 (2021).
45. Parveen, N. *et al.* Thermophysical properties of chemotactic microorganisms in bio-convective peristaltic rheology of nano-liquid with slippage, Joule heating and viscous dissipation. *Case Stud. Therm. Eng.* **27**, 101285 (2021).
46. Awais, M., Awan, S. E., Raja, M. A. Z. & Shoaib, M. Effects of Gyro-Tactic organisms in bio-convective nano-material with heat immersion, stratification, and viscous dissipation. *Arab. J. Sci. Eng.* **46**(6), 5907–5920 (2021).
47. Khan, W. U. *et al.* Analytical assessment of (Al_2O_3–Ag/H_2O) hybrid nanofluid influenced by induced magnetic field for second law analysis with mixed convection, viscous dissipation and heat generation. *Coatings* **11**(5), 498 (2021).
48. Awais, M. *et al.* Heat transfer in nanomaterial suspension (CuO and Al_2O_3) using KKL model. *Coatings* **11**(4), 417 (2021).
49. Awais, M. *et al.* Effects of variable transport properties on heat and mass transfer in MHD bioconvective nanofluid rheology with gyrotactic microorganisms: Numerical approach. *Coatings* **11**(2), 231 (2021).
50. Awan, S. E. *et al.* Numerical treatment for dynamics of second law analysis and magnetic induction effects on ciliary induced peristaltic transport of hybrid nanomaterial. *Front. Phys.* **9**, 631903 (2021).
51. Akhtar, R. *et al.* Analytical treatment for the dynamics of second law analysis of Jeffery nanofluid with convective heat and mass conditions. *J. Nanoelectron. Optoelectron.* **16**(1), 89–96 (2021).
52. Nazir, U., Nawaz, M. & Alharbi, S. O. Thermal performance of magnetohydrodynamic complex fluid using nano and hybrid nanoparticles. *Physica A* **553**, 124345 (2020).
53. Waini, I., Khan, U., Zaib, A., Ishak, A. & Pop, I. Inspection of TiO_2-$CoFe_2O_4$ nanoparticles on MHD flow toward a shrinking cylinder with radiative heat transfer. J. Mol. Liq., 119615 (2022).
54. Malik, M. Y. *et al.* Mixed convection dissipative viscous fluid flow over a rotating cone by way of variable viscosity and thermal conductivity. *Results Phys.* **6**, 1126–1135 (2016).

Author contributions

All the authors reviewed the manuscript and approved the submission.

Funding

This research is supported by Department of Mathematics, Faculty of Science, Khon Kaen University, Fiscal Year 2022.

Competing interests

The authors declare no competing interests.

Additional information

Correspondence and requests for materials should be addressed to K.M.

Reprints and permissions information is available at www.nature.com/reprints.

Publisher's note Springer Nature remains neutral with regard to jurisdictional claims in published maps and institutional affiliations.